



ARTICLE

MHD Maxwell Fluid with Heat Transfer Analysis under Ramp Velocity and Ramp Temperature Subject to Non-Integer Differentiable Operators

Thabet Abdeljawad^{1,2,3}, Muhammad Bilal Riaz^{4,5}, Syed Tauseef Saeed^{6,*} and Nazish Iftikhar⁶

¹Department of Mathematics and General Sciences, Prince Sultan University, Riyadh, 12435, Saudi Arabia

²Department of Medical Research, China Medical University, Taichung, 404, Taiwan

³Department of Computer Science and Information Engineering, Asia University, Taichung, 41354, Taiwan

⁴Department of Mathematics, University of Management and Technology, Lahore, 54770, Pakistan

⁵Institute for Groundwater Studies (IGS), University of the Free State, Bloemfontein, 9301, South Africa

⁶Department of Science & Humanities, National University of Computer and Emerging Sciences, Lahore, 54000, Pakistan

*Corresponding Author: Syed Tauseef Saeed. Email: tauseefsaeed301@gmail.com

Received: 03 July 2020 Accepted: 19 October 2020

ABSTRACT

The main focus of this study is to investigate the impact of heat generation/absorption with ramp velocity and ramp temperature on magnetohydrodynamic (MHD) time-dependent Maxwell fluid over an unbounded plate embedded in a permeable medium. Non-dimensional parameters along with Laplace transformation and inversion algorithms are used to find the solution of shear stress, energy, and velocity profile. Recently, new fractional differential operators are used to define ramped temperature and ramped velocity. The obtained analytical solutions are plotted for different values of emerging parameters. Fractional time derivatives are used to analyze the impact of fractional parameters (memory effect) on the dynamics of the fluid. While making a comparison, it is observed that the fractional-order model is best to explain the memory effect as compared to classical models. Our results suggest that the velocity profile decrease by increasing the effective Prandtl number. The existence of an effective Prandtl number may reflect the control of the thickness of momentum and enlargement of thermal conductivity. The incremental value of the M is observed for a decrease in the velocity field, which reflects to control resistive force. Further, it is noted that the Atangana-Baleanu derivative in Caputo sense (ABC) is the best to highlight the dynamics of the fluid. The influence of pertinent parameters is analyzed graphically for velocity and energy profile. Expressions for skin friction and Nusselt number are also derived for fractional differential operators.

KEYWORDS

MHD Maxwell fluid; fractional differential operator; heat generation absorption; thermal effect; non-singular kernels



1 Introduction

Viscoelasticity has important implications due to the characterization of viscoelastic parameters (relaxation and retardation phenomenon), elastic shearing strain, thermal relaxation, time-dependent an elastic aspect, and other rheological properties [1–3]. In such fluid, stress and rate of strain have a nonlinear relationship and enhance their order which makes the flow equation more complicated [4,5]. Elastic and memory effect for the flow of rate type fluid discussed by Maxwell.

Firstly, Maxwell [6] analyzed the visco-elastic attributes of air. Fetecau et al. [7] investigate the closed-form solution of the Maxwell model over an unbounded plate. Moreover, authors [8] discussed the Maxwell model over unbounded plate swing in the plane. Some significant results of the Maxwell model can be studied in [9–12]. Aman et al. [13] investigated the heat transfer analysis of Maxwell fluid flow with carbon nanotubes. The analytical solution of a Maxwell fluid with slip effects was investigated by Asif et al. [14]. Further, authors [15] discussed the unsteady rotational flow of Maxwell fluid in a Cylinder subject to shear stress. Noor [16] analyzed the impacts of chemical reaction on MHD Maxwell fluid flow for a vertical stretching sheet. In the literature, all the above-mentioned articles dealing with the flow of uniform and constant boundary conditions. There is an insufficient study that deals with flows under ramped wall temperature and ramped wall velocity conditions. Physically, the implementation of ramped wall velocity and temperature in real-life problems has a significant role. The diagnoses of prognosis, establishing treatments, analysis of heart functions, and blood vessel system [17–20] are major applications of ramp velocity. Firstly, the authors [21] discussed the simultaneous use of ramped velocity and temperature. Seth et al. [22–24] investigated heat and mass transfer phenomena with ramp temperature conditions. Recently, Tiwana et al. [25] and Anwar et al. [26] analyzed MHD Oldroyd-B fluid in the presence of thermal radiation under the effect of ramped temperature and ramped velocity. Anwar et al. [27] analyzed the flow of MHD Maxwell fluid under the impact of ramped wall temperature and velocity. Shah et al. [28] analyzed the convection flow of viscous fluids with analytical results by employing the time-fractional Caputo–Fabrizio derivative.

The technique of fractional calculus has been used to formulate mathematical modeling in various technological development, engineering applications, and industrial sciences. Different valuable work has been discussed for modeling fluid dynamics, signal processing, viscoelasticity, electrochemistry, and biological structure through fractional time derivatives. This fractional differential operator found useful conclusions for experts to treat cancer cells with a suitable amount of heat source and have compared the results to see the memory effect of temperature function. As compared to classical models, the memory effect is much stronger in fractional derivatives. From the past to the present, modeling of the different processes is handled through various types of fractional derivatives and fractal-fractional differential operators, such that Caputo (Power law), Atangana–Baleanu (Mittage–Leffler law), Caputo–Fabrizio (exponential law), Riemann–Liouville, modified Riemann–Liouville (Power law with boundaries) and few others [29–36]. Recently, Imran et al. [37] studied the comparison approach between Caputo–Fabrizio and Atangana–Baleanu fractional derivative and found that Atangana–Baleanu fractional derivative is excellent in exhibiting the memory effect in fluid flow problems. Convective flow with ramped wall temperature for non-singular kernel analyzed by Riaz et al. [38]. Further, Riaz et al. [39] discuss MHD Maxwell fluid with heat effect using local and non-local operators. Moreover, the authors [40] analyze the comparative study of heat transfer of MHD Maxwell fluid in view of fractional operators. Khan et al. [41,42] discussed the heat transfer analysis in

a Maxwell fluid using fractional Caputo-Fabrizio derivatives. Some recent studies related to the applications of modern techniques of fractional derivatives can be seen [43–48].

The main objective of this paper is to investigate the MHD Maxwell model with the definition of fractional order derivative in a Darcy medium. The solution of fluid velocity, energy, and shear stress are obtained by Caputo-Fabrizio (CF) and Atangana-Baleanu derivative in Caputo sense (ABC) fractional derivative models under influence of ramped velocity and temperature. These non-integer order derivatives are good for handling the mathematical calculation. Section 2 helps to derive the governing partial differential equations. The solution of the temperature profile, velocity profile, and shear stress can be achieved through CF and ABC fractional models with help of Laplace transformation and inversion algorithm in Sections 3 and 4 respectively. In Section 5, the influence of physical parameters is discussed graphically by MATHCAD-15 software. Finally, the conclusion of the present article is given at the end.

2 Development of Governing Equations Based on Problem Statement

Consider the MHD time-dependent Maxwell model over an unbounded vertical plate immersed in a permeable surface. The plate is along the x-axis, while the ξ -axis is perpendicular to the plate. At the wall end, both velocity and temperature have time-dependent conditions up to some certain limit of time known as the characteristic time; after that time, both velocity and temperature attain constant values u_0 and T_∞ . The physical model expressed in Fig. 1. Under these presumptions, the governing equation for MHD Maxwell fluid with appropriate conditions are given below [27,41]:

$$\left(1 + \lambda \frac{\partial}{\partial t}\right) \frac{\partial W(\xi, t)}{\partial t} = \nu \frac{\partial^2 W(\xi, t)}{\partial \xi^2} + g\beta \left(1 + \lambda \frac{\partial}{\partial t}\right) (T - T_\infty) - \left(\frac{\mu\phi}{\rho k^*} + \frac{\sigma B_0^2}{\rho}\right) \left(1 + \lambda \frac{\partial}{\partial t}\right) W(\xi, t), \tag{1}$$

$$\rho C_p \frac{\partial T(\xi, t)}{\partial t} = k \frac{\partial^2 T(\xi, t)}{\partial \xi^2} - \frac{\partial q_r}{\partial \xi} - Q_o T(\xi, t) + Q_o T_\infty(\xi, t), \tag{2}$$

$$\left(1 + \lambda \frac{\partial}{\partial t}\right) S = \mu \frac{\partial W(\xi, t)}{\partial \xi}. \tag{3}$$

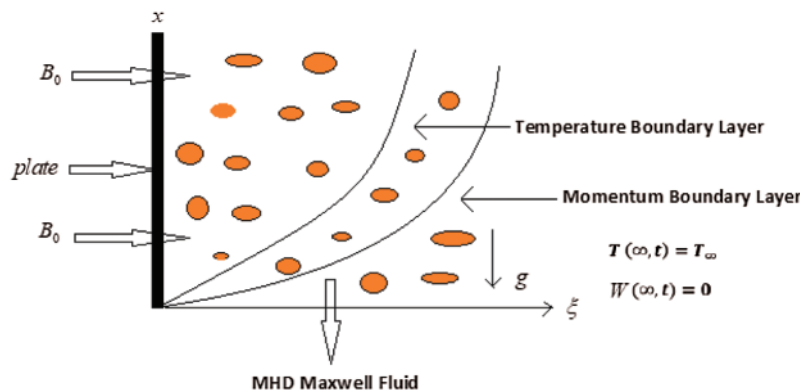


Figure 1: Geometrical presentation for MHD Maxwell model

Eqs. (1)–(3) represent as governing equations of velocity, energy and shear stress distributions respectively subject to imposed conditions as:

$$\xi \geq 0: \quad W(\xi, 0) = 0, \quad T(\xi, 0) = T_\infty, \quad W_t(\xi, 0) = 0, \quad W_\xi(\xi, 0) = 0, \quad (4)$$

$$W(0, t) = \begin{cases} U_o \frac{t}{t_0}, & 0 < t \leq t_0 \\ W(0, t) = U_o, & t > t_0, \end{cases}, \quad T(0, t) = \begin{cases} T_\infty + (T_w - T_\infty) \frac{t}{t_0}, & 0 < t \leq t_0 \\ T(0, t) = T_w, & t > t_0, \end{cases} \quad (5)$$

$$t \geq 0: \quad W(\xi, t) \rightarrow 0, T(\xi, t) \rightarrow T_\infty, \text{ as } \xi \rightarrow \infty. \quad (6)$$

Introduce dimensionless elements to form the problem free from geometric

$$\zeta = \frac{\xi U_o}{v}, \quad \tau = \frac{t U_o^2}{v}, \quad w = \frac{W}{U_o}, \quad \theta = \frac{T - T_\infty}{T_w - T_\infty}, \quad \lambda_1 = \frac{\lambda U_o^2}{v}, \quad P_r = \frac{\mu C_p}{k}, \quad \frac{1}{K} = \frac{\phi v^2}{k^* U_o^2}, \quad (7)$$

$$S_1 = \frac{S}{\rho U_o^2}, \quad t_0 = \frac{v}{U_o^2}, \quad G_r = \frac{g \beta v (T_w - T_\infty)}{U_o^3}, \quad M = \frac{\sigma B_o^2 v}{\rho U_o^2}, \quad Q = \frac{v Q_o}{\rho C_p U_o^2}, \quad N_r = \frac{16 \sigma_1 T_\infty^3}{3 k k^*}. \quad (8)$$

After simplification, we have the set of dimensionless governing equations:

$$\left(1 + \lambda_1 \frac{\partial}{\partial \tau}\right) \frac{\partial w(\zeta, \tau)}{\partial \tau} = \frac{\partial^2 w(\zeta, \tau)}{\partial \zeta^2} + G_r \left(1 + \lambda_1 \frac{\partial}{\partial \tau}\right) \theta(\zeta, \tau) - \left(M + \frac{1}{K}\right) \left(1 + \lambda_1 \frac{\partial}{\partial \tau}\right) w(\zeta, \tau), \quad (9)$$

$$\frac{\partial \theta(\zeta, \tau)}{\partial \tau} = \frac{1}{P_{\text{reff}}} \frac{\partial^2 \theta(\zeta, \tau)}{\partial \zeta^2} + Q \theta(\zeta, \tau), \quad (10)$$

$$\left(1 + \lambda_1 \frac{\partial}{\partial \tau}\right) S_1 = \frac{\partial w(\zeta, \tau)}{\partial \zeta}, \quad (11)$$

with corresponding conditions

$$\zeta \geq 0: \quad w(\zeta, 0) = 0, \quad \theta(\zeta, 0) = 0, \quad w_t(\zeta, 0) = w_\zeta(\zeta, 0) = 0, \quad (12)$$

$$w(0, \tau) = \theta(0, \tau) = \begin{cases} \tau & 0 < \tau \leq 1; = \tau H(\tau) - (\tau - 1)H(\tau - 1) \\ 1 & \tau > 1, \end{cases}, \quad (13)$$

$$\tau \geq 0: \quad w(\zeta, \tau) \rightarrow 0, \quad \theta(\zeta, \tau) \rightarrow 0, \text{ as } \zeta \rightarrow \infty. \quad (14)$$

3 Solution of Temperature Profile

3.1 Caputo–Fabrizio Fractional Derivative

Fractional operators are quite flexible for describing the behaviors of energy transfer of MHD Maxwell fluid through the characterization of governing equations. Generating fractional governing equation of temperature (10) via CF-fractional operator (16) by exchanging the partial time derivative with fractional derivative of order κ ,

$${}^{CF}D_{\tau}^{\kappa}\theta(\zeta, \tau) = \frac{1}{P_{\text{reff}}} \frac{\partial^2\theta(\zeta, \tau)}{\partial\zeta^2} + Q\theta(\zeta, \tau), \tag{15}$$

where, ${}^{CF}D_{\tau}^{\kappa}$ is known as CF fractional operator [32] is defined by

$${}^{CF}D_{\tau}^{\kappa}N(\zeta, \tau) = \frac{1}{1-\kappa} \int_0^{\tau} \exp\left(-\frac{\kappa(\tau-\xi)}{1-\kappa}\right) N'(\xi) d\xi, \quad 0 < \kappa < 1. \tag{16}$$

Solving the uncoupled and fractionalized governing equation of temperature (15) by Laplace transform method. One has to need the following typical property of Caputo–Fabrizio fractional operator defined in Eq. (17)

$$\mathcal{L}\left({}^{CF}D_{\tau}^{\kappa}N(\zeta, \tau)\right) = \frac{s\mathcal{L}(N(\zeta, \tau)) - N(\zeta, 0)}{(1-\kappa)s + \kappa}, \tag{17}$$

employing Laplace transformation on (15) with the help of (17), we explored second order partial differential equation

$$\frac{\partial^2\bar{\theta}_{cf}(\zeta, s)}{\partial\zeta^2} - P_{\text{reff}}\left(\frac{s}{(1-\kappa)s + \kappa} + Q\right)\bar{\theta}_{cf}(\zeta, s) = 0. \tag{18}$$

More suitable form of temperature field is

$$\frac{\partial^2\bar{\theta}_{cf}(\zeta, s)}{\partial\zeta^2} - P_{\text{reff}}\left(\frac{g_1s + g_2}{g_3s + g_4}\right)\bar{\theta}_{cf}(\zeta, s) = 0. \tag{19}$$

The solution of homogenous part of second order partial differential equation say (19) is,

$$\bar{\theta}_{cf}(\zeta, s) = c_1 e^{-\zeta\sqrt{P_{\text{reff}}\left(\frac{g_1s + g_2}{g_3s + g_4}\right)}} + c_2 e^{\zeta\sqrt{P_{\text{reff}}\left(\frac{g_1s + g_2}{g_3s + g_4}\right)}}, \tag{20}$$

with the help of Eqs. (12)–(14), we find out the values of constants c_1 and c_2 for temperature equation

$$\bar{\theta}_{cf}(\zeta, s) = \left(\frac{1 - e^{-s}}{s^2}\right) e^{-\zeta\sqrt{P_{\text{reff}}\left(\frac{g_1s + g_2}{g_3s + g_4}\right)}}, \tag{21}$$

where

$$g_1 = 1 + Q - \kappa Q, \quad g_2 = \kappa Q, \quad g_3 = 1 - \kappa, \quad g_4 = \kappa.$$

The expression of Nusselt number Nu for CF differentiation is given as:

$$Nu_{cf} = -\frac{\partial \theta}{\partial \zeta}(0, \tau) = \mathcal{L}^{-1} \left(\sqrt{P_{reff} \left(\frac{g_1 s + g_2}{g_3 s + g_4} \right)} \times \left(\frac{1 - e^{-s}}{s^2} \right) \right). \quad (22)$$

3.2 Atangana–Baleanu Fractional Derivative

Generating a fractional governing equation of temperature (15) via ABC-fractional operator (24) by exchanging the partial time derivative with fractional derivative of order γ ,

$${}^{ABC}D_{\tau}^{\gamma} \theta(\zeta, \tau) = \frac{1}{P_{reff}} \frac{\partial^2 \theta(\zeta, \tau)}{\partial \zeta^2} + Q \theta(\zeta, \tau), \quad (23)$$

where ${}^{ABC}D_{\tau}^{\gamma}$ is known as ABC fractional operator [33] is defined by

$${}^{ABC}D_{\tau}^{\alpha} f(\xi, \tau) = \frac{M(\alpha)}{1-\alpha} \int_0^{\tau} \mathbf{E}_{\alpha} \left(-\frac{\alpha(t-\tau)^{\alpha}}{1-\alpha} \right) \frac{\partial f(\xi, \tau)}{\partial \tau} d\tau, \quad \text{with } \sum_{m=0}^{\infty} \frac{(-t)^{\alpha m}}{\Gamma(1+\alpha m)} = \mathbf{E}_{\alpha}(-t)^{\alpha}, \quad (24)$$

where $M(\alpha)$ denotes a normalization function obeying $M(0) = M(1) = 1$.

Solving governing equation of temperature (23) by Laplace transform method. One has to need the following typical property of ABC-fractional operator defined in Eq. (25)

$$\mathcal{L} \left({}^{ABC}D_{\tau}^{\alpha} f(\xi, t) \right) = \frac{s^{\alpha} \mathcal{L}(f(\xi, t)) - s^{\alpha-1} f(\xi, 0)}{(1-\alpha)s^{\alpha} + \alpha}, \quad (25)$$

employing Laplace transformation on (23) with the help of (25), we explored second order partial differential equation:

$$\frac{\partial^2 \bar{\theta}_{abc}(\zeta, s)}{\partial \zeta^2} - P_{reff} \left(\frac{s^{\gamma}}{(1-\gamma)s^{\gamma} + \gamma} + Q \right) \bar{\theta}_{abc}(\zeta, s) = 0. \quad (26)$$

More suitable form of temperature field is,

$$\frac{\partial^2 \bar{\theta}_{abc}(\zeta, s)}{\partial \zeta^2} - P_{reff} \left(\frac{h_1 s^{\gamma} + h_2}{h_3 s^{\gamma} + h_4} \right) \bar{\theta}_{abc}(\zeta, s) = 0, \quad (27)$$

The solution of homogenous part of second order partial differential equation say (27),

$$\bar{\theta}_{abc}(\zeta, s) = c_1 e^{-\zeta \sqrt{P_{reff} \left(\frac{h_1 s^{\gamma} + h_2}{h_3 s^{\gamma} + h_4} \right)}} + c_2 e^{\zeta \sqrt{P_{reff} \left(\frac{h_1 s^{\gamma} + h_2}{h_3 s^{\gamma} + h_4} \right)}}, \quad (28)$$

with the help of Eqs. (12)–(14), we find out the values of constants c_1 and c_2 for temperature equation:

$$\bar{\theta}_{abc}(\zeta, s) = \left(\frac{1 - e^{-s}}{s^2} \right) e^{-\zeta \sqrt{P_{reff} \left(\frac{h_1 s^{\gamma} + h_2}{h_3 s^{\gamma} + h_4} \right)}}, \quad (29)$$

where

$$h_1 = 1 + Q - \gamma Q, \quad h_2 = \gamma Q, \quad h_3 = 1 - \gamma, \quad h_4 = \gamma.$$

The expression of Nusselt number Nu for ABC differentiation is given as:

$$Nu_{abc} = -\frac{\partial \theta}{\partial \zeta}(0, \tau) = \mathcal{L}^{-1} \left(\sqrt{P_{reff} \left(\frac{h_1 s^\gamma + h_2}{h_3 s^\gamma + h_4} \right)} \times \left(\frac{1 - e^{-s}}{s^2} \right) \right). \quad (30)$$

4 Solution of Velocity Profile

4.1 Caputo-Fabrizio Fractional Derivative

Generating a fractional governing equation of velocity Eq. (9) via CF-fractional operator say equation Eq. (16) by exchanging the partial time derivative with fractional derivative of order κ then solving the governing equation Eq. (9) by Laplace transform method, we get

$$\left(\left(1 + \frac{\lambda_1 s}{(1-\kappa)s + \kappa} \right) \left(s + M + \frac{1}{K} \right) \right) \bar{w}_{cf}(\zeta, s) = \frac{\partial^2 \bar{w}_{cf}(\zeta, s)}{\partial \zeta^2} + G_r \left(1 + \frac{\lambda_1 s}{(1-\kappa)s + \kappa} \right) \bar{\theta}_{cf}(\zeta, s). \quad (31)$$

The required homogeneous part of the Eq. (31) is given as:

$$\bar{w}_h(\zeta, s) = c_1 e^{-\zeta \sqrt{\left(s + M + \frac{1}{K}\right) \left(\frac{g_5 s + g_4}{g_3 s + g_4}\right)}} + c_2 e^{\zeta \sqrt{\left(s + M + \frac{1}{K}\right) \left(\frac{g_5 s + g_4}{g_3 s + g_4}\right)}}, \quad (32)$$

and particular solution can be give as follow after making use of Eq. (18),

$$\bar{w}_p(\zeta, s) = \frac{G_r (1 - e^{-s}) (g_5 s + g_4)}{g_5 s^2 (s^2 + g_8 s + g_9)} e^{-\zeta \sqrt{P_{reff} \left(\frac{g_1 s + g_2}{g_3 s + g_4}\right)}}, \quad (33)$$

and solution of Eq. (31) can be given as follow:

$$\bar{w}_{cf}(\zeta, s) = \bar{w}_h(\zeta, s) + \bar{w}_p(\zeta, s), \quad (34)$$

$$\begin{aligned} \bar{w}_{cf}(\zeta, s) = & c_1 e^{-\zeta \sqrt{\left(s + M + \frac{1}{K}\right) \left(\frac{g_5 s + g_4}{g_3 s + g_4}\right)}} + c_2 e^{\zeta \sqrt{\left(s + M + \frac{1}{K}\right) \left(\frac{g_5 s + g_4}{g_3 s + g_4}\right)}} \\ & + \frac{G_r (1 - e^{-s}) (g_5 s + g_4)}{g_5 s^2 (s^2 + g_8 s + g_9)} e^{-\zeta \sqrt{P_{reff} \left(\frac{g_1 s + g_2}{g_3 s + g_4}\right)}}, \end{aligned} \quad (35)$$

using conditions given in Eqs. (12)–(14) for velocity in order to find constants, we have

$$\begin{aligned} \bar{w}_{cf}(\zeta, s) = & \left(\frac{1 - e^{-s}}{s^2} \right) e^{-\zeta \sqrt{\left(s + M + \frac{1}{K}\right) \left(\frac{g_5 s + g_4}{g_3 s + g_4}\right)}} + \frac{G_r (1 - e^{-s}) (g_5 s + g_4)}{g_5 s^2 (s^2 + g_8 s + g_9)} \\ & \times \left(e^{-\zeta \sqrt{P_{reff} \left(\frac{g_1 s + g_2}{g_3 s + g_4}\right)}} - e^{-\zeta \sqrt{\left(s + M + \frac{1}{K}\right) \left(\frac{g_5 s + g_4}{g_3 s + g_4}\right)}} \right). \end{aligned} \quad (36)$$

The suitable and simplified form for inversion algorithm, we have

$$\bar{w}_{cf}(\zeta, s) = \left(\frac{1 - e^{-s}}{s^2} \right) \bar{Z}(\zeta, s), \quad (37)$$

and

$$\bar{Z}(\zeta, s) = e^{-\zeta \sqrt{\left(s+M+\frac{1}{K}\right)\left(\frac{g_5s+g_4}{g_3s+g_4}\right)}} + \frac{G_r}{g_5} \left(\frac{D_1}{s+B_1} + \frac{D_2}{s+B_2} \right) \left(e^{-\zeta \sqrt{P_{\text{reff}}\left(\frac{g_1s+g_2}{g_3s+g_4}\right)}} - e^{-\zeta \sqrt{\left(s+M+\frac{1}{K}\right)\left(\frac{g_5s+g_4}{g_3s+g_4}\right)}} \right), \quad (38)$$

where, letting parameters are described as

$$g_5 = 1 + \lambda_1 - \kappa, \quad g_6 = g_4 + \frac{g_5}{K} + g_5M - g_1P_{\text{reff}}, \quad g_7 = \frac{g_4}{K} + g_4M - g_2P_{\text{reff}}, \quad g_8 = \frac{g_6}{g_5}, \quad g_9 = \frac{g_7}{g_5},$$

$$g_{10} = \sqrt{\frac{g_8^2 - 4g_9}{4}}, \quad B_1 = \frac{g_8}{2} - g_{10}, \quad B_2 = \frac{g_8}{2} + g_{10}, \quad D_1 = \frac{-g_5g_8 + 2g_{10}g_5 + 2g_4}{4g_{10}},$$

$$D_2 = \frac{g_5g_8 + 2g_{10}g_5 - 2g_4}{4g_{10}}.$$

Differentiate Eq. (37) with respect to ζ , we have

$$\bar{w}_{cf}(\zeta, s) = \left(\frac{1 - e^{-s}}{s^2} \right) \frac{\partial \bar{Z}(\zeta, s)}{\partial \zeta}, \quad (39)$$

where

$$\begin{aligned} \frac{\partial \bar{Z}(\zeta, s)}{\partial \zeta} &= \sqrt{\left(s+M+\frac{1}{K}\right)\left(\frac{g_5s+g_4}{g_3s+g_4}\right)} e^{\zeta \sqrt{\left(s+M+\frac{1}{K}\right)\left(\frac{g_5s+g_4}{g_3s+g_4}\right)}} + \frac{G_r}{g_5} \left(\frac{D_1}{s+B_1} + \frac{D_2}{s+B_2} \right) \\ &\times \left(\sqrt{P_{\text{reff}}\left(\frac{g_1s+g_2}{g_3s+g_4}\right)} \right) e^{-\zeta \sqrt{P_{\text{reff}}\left(\frac{g_1s+g_2}{g_3s+g_4}\right)}} - \frac{G_r}{g_5} \left(\frac{D_1}{s+B_1} + \frac{D_2}{s+B_2} \right) \\ &\times \left(\sqrt{\left(s+M+\frac{1}{K}\right)\left(\frac{g_5s+g_4}{g_3s+g_4}\right)} \right) e^{\zeta \sqrt{\left(s+M+\frac{1}{K}\right)\left(\frac{g_5s+g_4}{g_3s+g_4}\right)}}. \end{aligned} \quad (40)$$

Plugging Eq. (38) into Eq. (11) gives the resultant solution of shear stress

$$\bar{S}_1(\zeta, s) = \left(\frac{g_3s+g_4}{g_5s+g_4} \right) \left(\frac{1 - e^{-s}}{s^2} \right) \frac{\partial \bar{Z}(\zeta, s)}{\partial \zeta}. \quad (41)$$

The expression of skin friction S_f for CF differentiation is given as:

$$S_{f_{cf}} = -\frac{\partial w(0, \tau)}{\partial \zeta} = \mathcal{L}^{-1} \left(\frac{1 - e^{-s}}{s^2} \times \frac{\partial \bar{Z}(0, s)}{\partial \zeta} \right). \quad (42)$$

4.2 Atangana-Baleanu Fractional Derivative

Generating a fractional governing equation of velocity Eq. (9) via ABC-fractional operator say equation Eq. (24) by exchanging the partial time derivative with fractional derivative of order γ then solving the governing equation Eq. (9) by Laplace transform method, we get

$$\left(\left(1 + \frac{\lambda_1 s^\gamma}{(1-\gamma)s^\gamma + \gamma} \right) \left(s + M + \frac{1}{K} \right) \right) \bar{w}_{abc}(\zeta, s) = \frac{\partial^2 \bar{w}_{abc}(\zeta, s)}{\partial \zeta^2} + G_r \left(1 + \frac{\lambda_1 s^\gamma}{(1-\gamma)s^\gamma + \gamma} \right) \bar{\theta}_{abc}(\zeta, s). \tag{43}$$

The homogeneous part of the Eq. (43) is given as:

$$\bar{w}_h(\zeta, s) = c_1 e^{-\zeta \sqrt{\left(s+M+\frac{1}{K}\right)\left(\frac{h_5 s^\gamma+h_4}{h_3 s^\gamma+h_4}\right)}} + c_2 e^{\zeta \sqrt{\left(s+M+\frac{1}{K}\right)\left(\frac{h_5 s^\gamma+h_4}{h_3 s^\gamma+h_4}\right)}}, \tag{44}$$

and particular solution can be give as follow after making use of Eq. (29) for the values $\bar{\theta}_{abc}(\zeta, s)$,

$$\bar{w}_p(\zeta, s) = \frac{G_r (1 - e^{-s}) (h_5 s^\gamma + h_4)}{h_5 s^2 (s^{2\gamma} + h_8 s^\gamma + h_9)} e^{-\zeta \sqrt{P_{reff} \left(\frac{h_1 s^\gamma+h_2}{h_3 s^\gamma+h_4}\right)}}, \tag{45}$$

using conditions given in Eqs. (9)–(11) for velocity in order to find constants, we have

$$\begin{aligned} \bar{w}_{abc}(\zeta, s) &= \left(\frac{1 - e^{-s}}{s^2} \right) e^{-\zeta \sqrt{\left(s+M+\frac{1}{K}\right)\left(\frac{h_5 s^\gamma+h_4}{h_3 s^\gamma+h_4}\right)}} + \frac{G_r (1 - e^{-s}) (h_5 s^\gamma + h_4)}{h_5 s^2 (s^{2\gamma} + h_8 s^\gamma + h_9)} \\ &\times \left(e^{-\zeta \sqrt{P_{reff} \left(\frac{h_1 s^\gamma+h_2}{h_3 s^\gamma+h_4}\right)}} - e^{-\zeta \sqrt{\left(s+M+\frac{1}{K}\right)\left(\frac{h_5 s^\gamma+h_4}{h_3 s^\gamma+h_4}\right)}} \right). \end{aligned} \tag{46}$$

The suitable and simplified form for inversion algorithm, we have

$$\bar{w}_{abc}(\zeta, s) = \left(\frac{1 - e^{-s}}{s^2} \right) \bar{H}(\zeta, s), \tag{47}$$

and

$$\begin{aligned} \bar{H}(\zeta, s) &= e^{-\zeta \sqrt{\left(s+M+\frac{1}{K}\right)\left(\frac{h_5 s^\gamma+h_4}{h_3 s^\gamma+h_4}\right)}} + \frac{G_r}{h_5} \left(\frac{D_3}{s^\gamma + B_3} + \frac{D_4}{s^\gamma + B_4} \right) \\ &\times \left(e^{-\zeta \sqrt{P_{reff} \left(\frac{h_1 s^\gamma+h_2}{h_3 s^\gamma+h_4}\right)}} - e^{-\zeta \sqrt{\left(s+M+\frac{1}{K}\right)\left(\frac{h_5 s^\gamma+h_4}{h_3 s^\gamma+h_4}\right)}} \right), \end{aligned} \tag{48}$$

where, letting parameters are described as

$$h_5 = 1 + \lambda_1 - \gamma, \quad h_6 = h_4 + \frac{h_5}{K} + h_5 M - h_1 P_{reff}, \quad h_7 = \frac{h_4}{K} + h_4 M - h_2 P_{reff}, \quad h_8 = \frac{h_6}{h_5}, \quad h_9 = \frac{h_7}{h_5},$$

$$h_{10} = \sqrt{\frac{h_8^2 - 4h_9}{4}}, \quad B_3 = \frac{h_8}{2} - h_{10}, \quad B_4 = \frac{h_8}{2} + h_{10}, \quad D_3 = \frac{-h_5h_8 + 2h_{10}h_5 + 2h_4}{4h_{10}},$$

$$D_4 = \frac{h_5h_8 + 2h_{10}h_5 - 2h_4}{4h_{10}}.$$

Differentiate Eq. (47) with respect to ζ , we have

$$\bar{w}_{abc}(\zeta, s) = \left(\frac{1 - e^{-s}}{s^2} \right) \frac{\partial \bar{H}(\zeta, s)}{\partial \zeta}, \quad (49)$$

where

$$\begin{aligned} \frac{\partial \bar{H}(\zeta, s)}{\partial \zeta} = & \sqrt{\left(s + M + \frac{1}{K}\right) \left(\frac{h_5s^\gamma + h_4}{h_3s^\gamma + h_4}\right)} e^{-\zeta \sqrt{\left(s + M + \frac{1}{K}\right) \left(\frac{h_5s^\gamma + h_4}{h_3s^\gamma + h_4}\right)}} + \frac{G_r}{h_5} \left(\frac{D_3}{s^\gamma + B_3} + \frac{D_4}{s^\gamma + B_4} \right) \\ & \times \left(\sqrt{P_{\text{reff}} \left(\frac{h_1s^\gamma + h_2}{h_3s^\gamma + h_4} \right)} \right) e^{-\zeta \sqrt{P_{\text{reff}} \left(\frac{h_1s^\gamma + h_2}{h_3s^\gamma + h_4} \right)}} - \frac{G_r}{h_5} \left(\frac{D_3}{s^\gamma + B_3} + \frac{D_4}{s^\gamma + B_4} \right) \\ & \times \left(\sqrt{\left(s + M + \frac{1}{K}\right) \left(\frac{h_5s^\gamma + h_4}{h_3s^\gamma + h_4}\right)} \right) e^{-\zeta \sqrt{\left(s + M + \frac{1}{K}\right) \left(\frac{h_5s^\gamma + h_4}{h_3s^\gamma + h_4}\right)}}. \end{aligned} \quad (50)$$

Plugging Eq. (50) into Eq. (11) gives the resultant solution of shear stress:

$$\bar{S}_1(\zeta, s) = \left(\frac{h_3s^\gamma + h_4}{h_5s^\gamma + h_4} \right) \left(\frac{1 - e^{-s}}{s^2} \right) \frac{\partial \bar{H}(\zeta, s)}{\partial \zeta}. \quad (51)$$

The expression of skin friction S_f for ABC differentiation is given as:

$$S_{f_{cf}} = -\frac{\partial w(0, \tau)}{\partial \zeta} = \mathcal{L}^{-1} \left(\frac{1 - e^{-s}}{s^2} \times \frac{\partial \bar{H}(0, s)}{\partial \zeta} \right). \quad (52)$$

In our flow models we use classical computational technique (Laplace transform) to solve the given models using different definitions of fractional derivatives. There are many algorithms for the numerical calculation of the inverse Laplace transform. The Stehfest's formula, which approximates the inverse Laplace transform is simple, easy to use compared with other algorithms. In this paper we use Stehfest's algorithm and also give comparison with other in tabular form. Tzou's calculation for approval of our numerical inverse Laplace

$$v(r, t) = \frac{e^{4.7}}{t} \left[\frac{1}{2} \bar{v} \left(r, \frac{4.7}{t} \right) + \text{Re} \left\{ \sum_{k=1}^{N_1} (-1)^k \bar{v} \left(r, \frac{4.7 + k\pi i}{t} \right) \right\} \right],$$

where $\text{Re}(\cdot)$ is the real part, i is the imaginary unit and N_1 is a natural number [49,50].

5 Results and Discussion

This section is dedicated to present physical interpretation of the obtained results via CF and AB differential operators under heat generation, ramp velocity, and ramp temperature on the MHD Maxwell model. Results are investigated via Laplace transformation with an inversion algorithm for velocity, energy, and shear stress based on singular versus non-singular and local versus non-local kernels. The graphical representations are depicted for showing the influences of different physical parameters such as effective Prandtl number P_{reff} , thermal Grashof number G_r , fractional parameters γ and magnetic effect M on velocity and energy profile using the package of MATHCAD-15. Additionally, we focus our depicted graphs for the comparison of ramped temperature with constant temperature using a fractional operator.

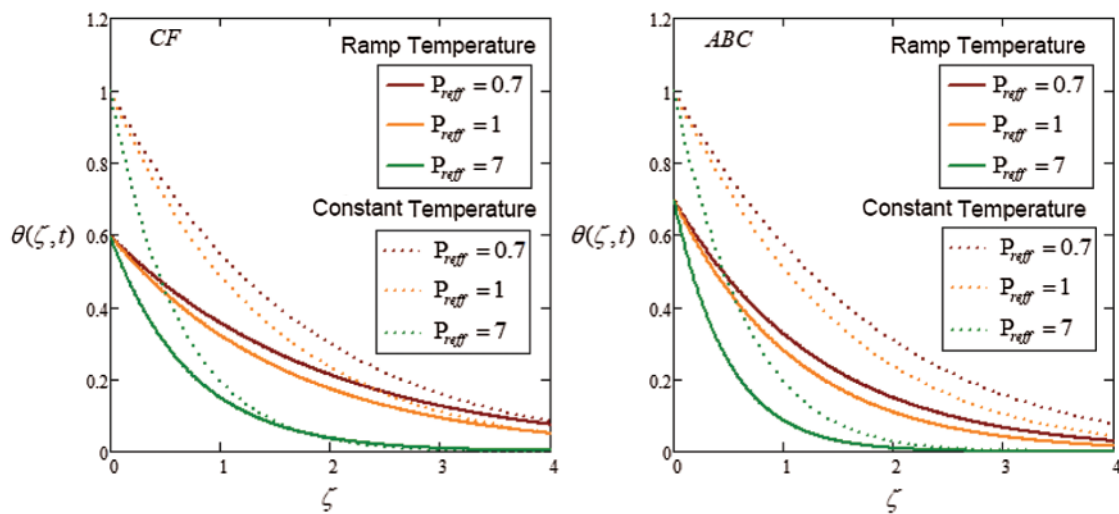


Figure 2: Plot via CF and AB-approaches for temperature with variation of P_{reff} and time

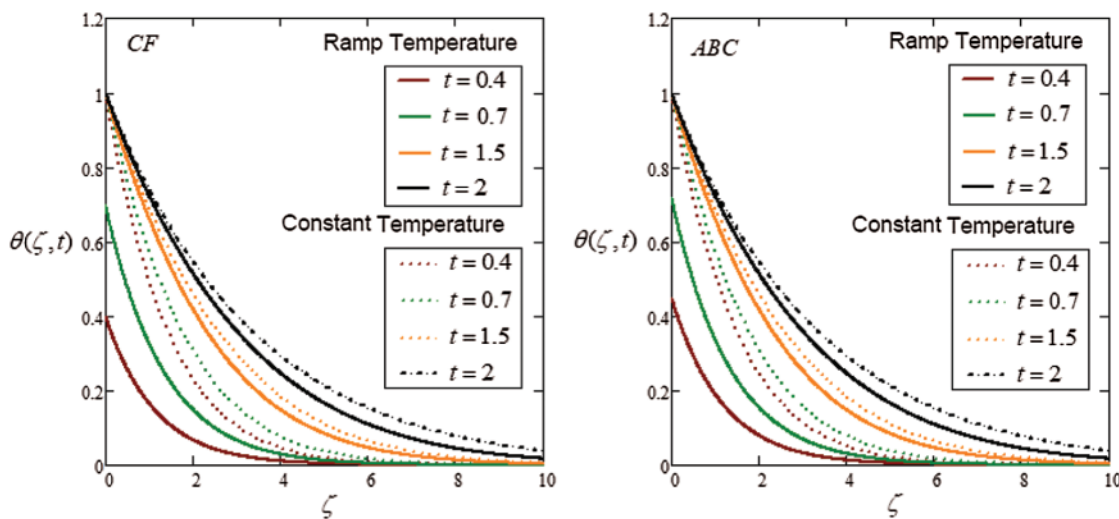


Figure 3: Plot via CF and AB-approaches for temperature with different values of time effect

Fig. 2 is plotted for the impact of P_{reff} on the energy profile. It is seen that the thermal layer and temperature decrease by a large value of P_{reff} . As P_{reff} increases, the temperature profile reduces more rapidly on the ABC model as compared to the CF model. Physically, for a small value of P_{reff} thermal conductivity enhances which allows heat to diffuse away rapidly for a higher value of P_{reff} . For the isothermal case, the energy solution has a higher profile. The influence of time on the temperature field can be analyzed in Fig. 3. For CF and ABC models, as an increase in time effect the resultant energy profile reduces for both ramped and isothermal wall conditions.

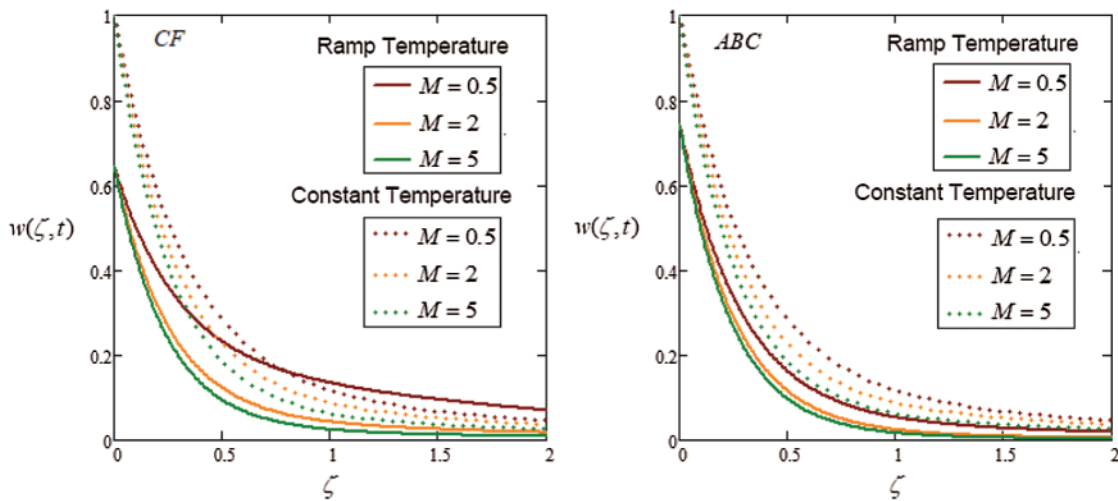


Figure 4: Plot via CF and AB-approaches for velocity with variation of time and M

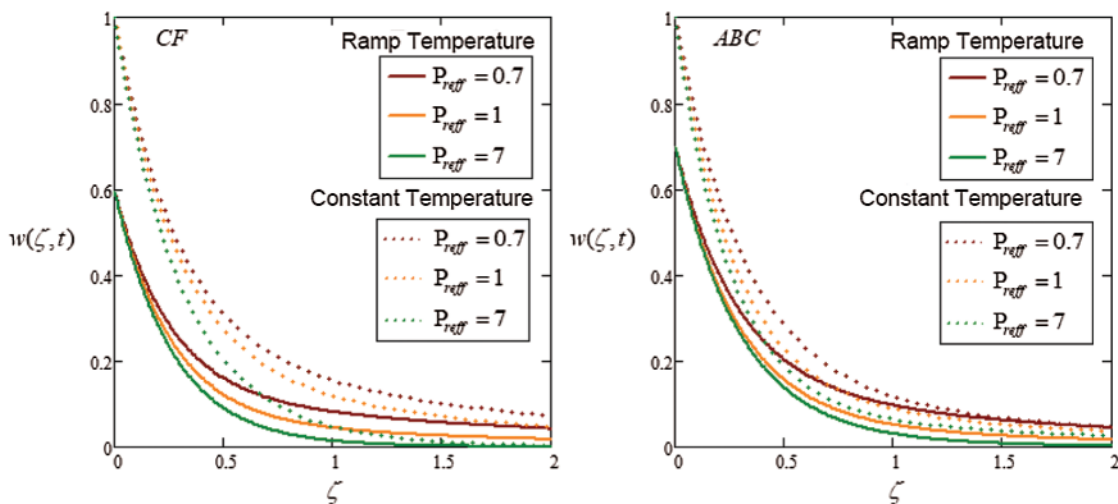


Figure 5: Plot via CF and AB-approaches for velocity with variation of time and P_{reff}

Fig. 4 investigates the influence of M on velocity components. This graphical representation indicates that an increase in the magnetic field, the velocity reduce due to Lorentz force. It behaves as a drag force. By increasing the parameter of the magnetic field, the Lorentz force also increases. Fluid flow on the boundary layer is slow down due to this force. Fig. 5 investigates the behavior of P_{reff} . Specific heat and conductivity depend on P_{reff} . The thickness of the momentum and boundary layer is control by an effective Prandtl number. It is seen from the graph, decreasing the velocity, observed by increase the value of P_{reff} . The lower effective Prandtl number enhances thermal conductivity and increase the boundary layer.

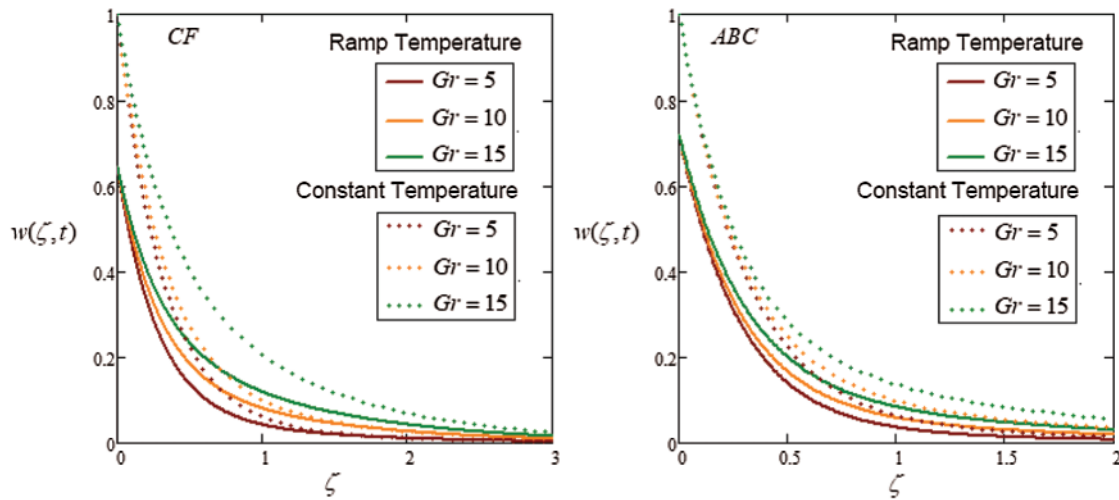


Figure 6: Plot via CF and AB-approaches for velocity with variation of time and G_r

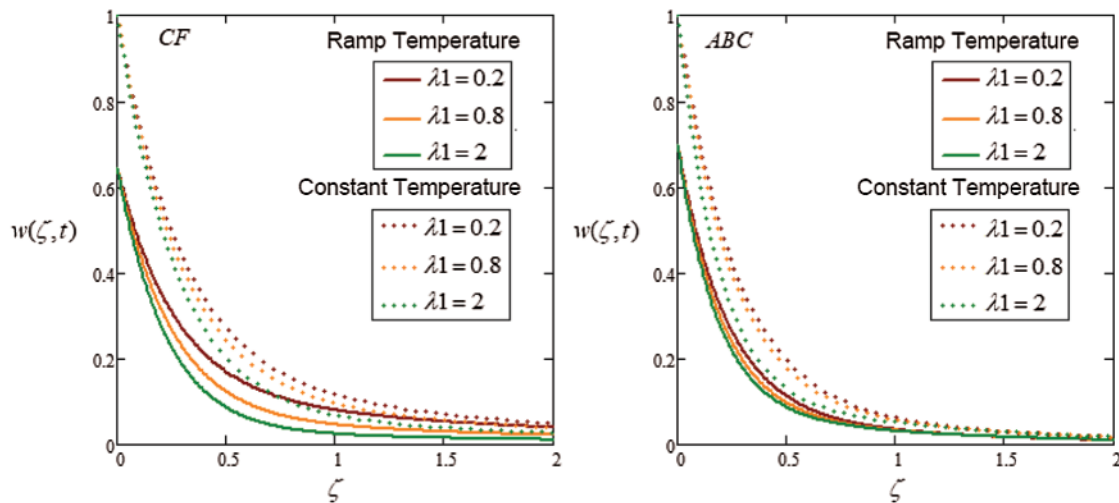


Figure 7: Plot via CF and AB-approaches for velocity with variation of time and λ_1

Fig. 6 shows that the impact on G_r for the velocity field versus time. It is the ratio of the buoyancy to a viscous force acting on the fluid. It can be seen in the velocity field enhance by increasing in G_r . In a physical sense, as expected, when the Grashof number is increased, then fluid flow rises due to the thermal buoyancy effects. The velocity for the ABC model is good as compare to CF models. It is observed that velocity for the isothermal condition is always larger than ramped conditions. Fig. 7 analyzes the unique role of λ_1 for ramped wall and isothermal wall conditions. The value of λ_1 enhances leads to reduce in velocity. In the physical sense, relaxation describes the return of a perturbed system to a state of equilibrium.

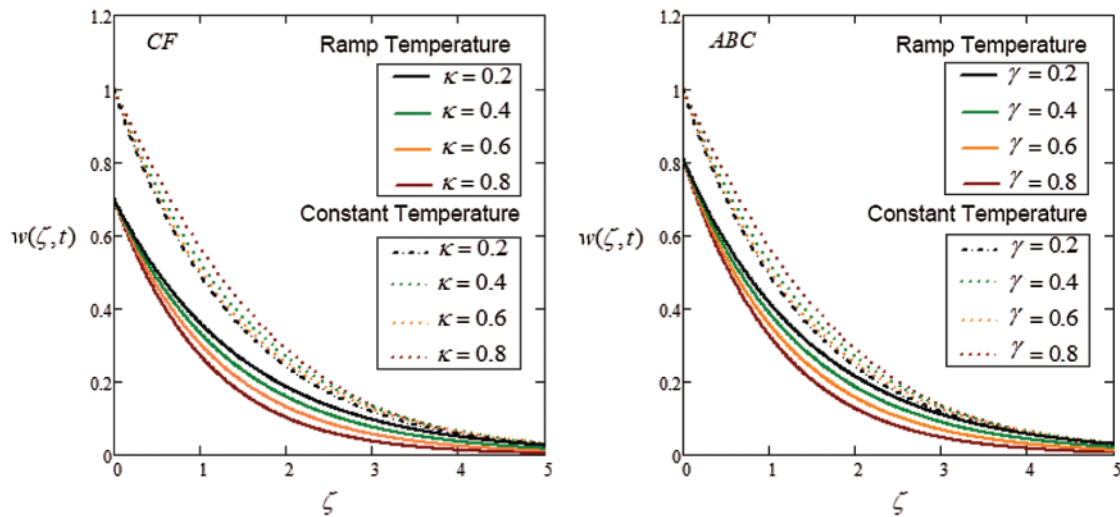


Figure 8: Plot via CF and AB-approaches for velocity with variation of time and γ

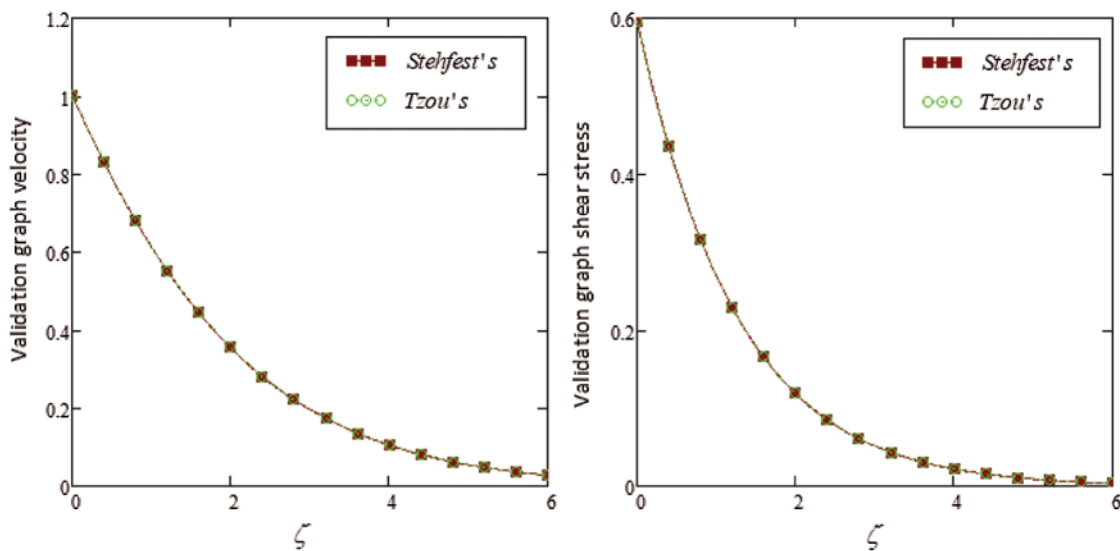


Figure 9: Comparison via Stehfest's and Tzou's algorithm

The influence of α on the velocity field can be analyzed in Fig. 8. The velocity field reduces by increasing the value of α for both *ABC* and *CF* models. The flow behavior for isothermal and ramped conditions are the same in all cases. To validate our solutions obtained by means of numerical inversion Laplace transform namely, Stehfest's and Tzou's algorithm. We represent the equivalence relation between those techniques in Fig. 9.

Fig. 10 is plotted to see the validity of our obtained results. We have compared our temperature results with the results from the studies by [26,27]. In Fig. 11, our obtained results are compared with the results of [22,26].

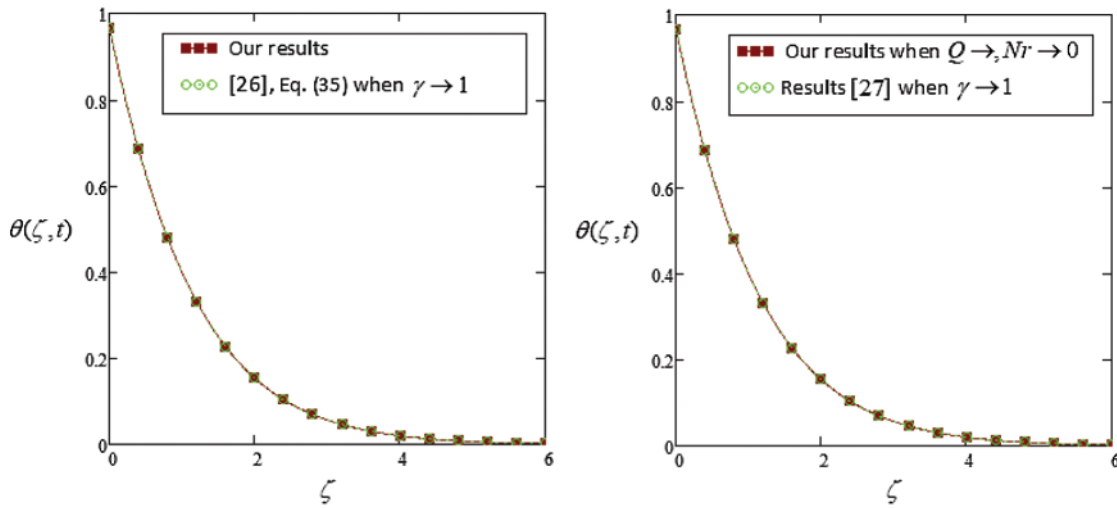


Figure 10: Temperature profile of our models compared with [26,27]

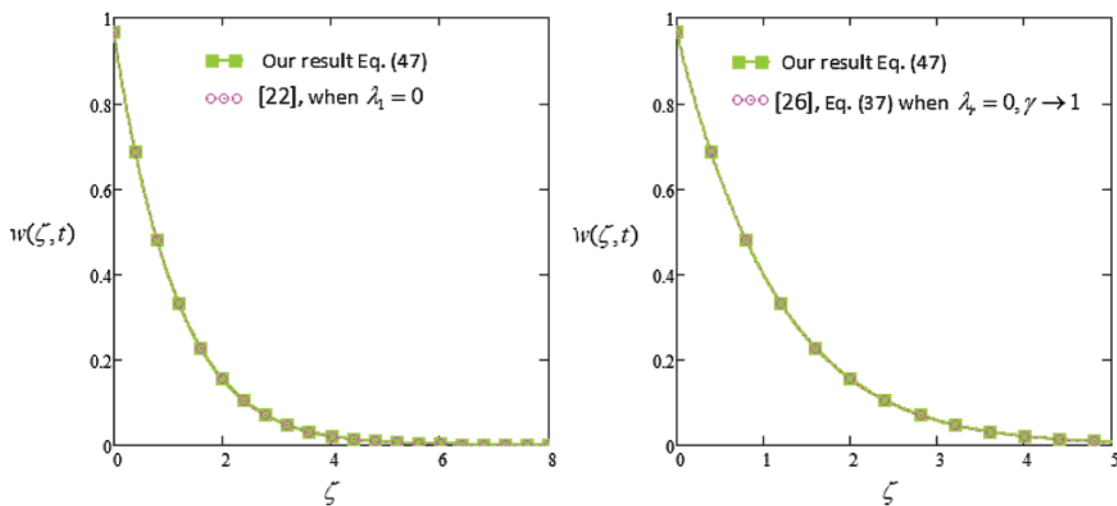


Figure 11: Velocity profile of our models compared with [26,27]

Tabs. 1 and **2** represent a comparison of the temperature profile between *CF* and *ABC* using Stehfest's and Tzou's algorithms with a variation of P_{reff} . It is observed that the temperature profile reduces with large values of P_{reff} . It is noted that the temperature is maximum in the *ABC* model as compared to *CF*. **Tabs. 3** and **4** represent a comparison of the fluid velocity between *CF* and *ABC* for increasing values of ζ by using inversion algorithms. Velocity increases for all models. The velocity obtained via the *ABC* approach is greater than the velocity computed with the help of the *CF* approach. Some numerical calculations for the Nusselt number for P_{reff} have been carried out by Stehfest's and Tzou's algorithms in **Tabs. 5** and **6**. It can be seen that the rate of heat transfer rate is high for the *ABC* model as compare to other models.

Table 1: Numerical inversion Laplace transform for temperature by Stehfest's and Tzou's

P_{reff}	Temperature (CF) [Stehfest's]	Temperature (CF) [Tzou's]
1	0.074	0.071
2	0.068	0.063
3	0.055	0.051
4	0.044	0.040
5	0.039	0.037
6	0.035	0.033
7	0.026	0.023
8	0.024	0.021
9	0.016	0.017
10	0.014	0.013

Table 2: Numerical inversion Laplace transform for temperature by Stehfest's and Tzou's

P_{reff}	Temperature (ABC) [Stehfest's]	Temperature (ABC) [Tzou's]
1	0.088	0.083
2	0.069	0.065
3	0.067	0.061
4	0.057	0.054
5	0.045	0.041
6	0.036	0.034
7	0.029	0.027
8	0.025	0.022
9	0.019	0.018
10	0.015	0.012

Table 3: Numerical inversion Laplace transform for velocity by Stehfest's and Tzou's

ζ	Velocity (CF) [Stehfest's]	Velocity (CF) [Tzou's]
0.2	0.978	0.965
0.4	0.921	0.925
0.6	0.876	0.879
0.8	0.833	0.821
1.0	0.791	0.782
1.2	0.752	0.731
1.4	0.713	0.708
1.6	0.677	0.663
1.8	0.641	0.628
2.0	0.617	0.609

Table 4: Numerical inversion Laplace transform for velocity by Stehfest's and Tzou's

ζ	Velocity (ABC) [Stehfest's]	Velocity (ABC) [Tzou's]
0.2	0.957	0.946
0.4	0.924	0.913
0.6	0.883	0.881
0.8	0.843	0.839
1.0	0.805	0.799
1.2	0.768	0.759
1.4	0.732	0.724
1.6	0.698	0.685
1.8	0.665	0.657
2.0	0.634	0.621

Table 5: Numerical inversion Laplace transform for Nusselt number by Stehfest's and Tzou's

P_{ref}	Nu (CF) [Stehfest's]	Nu (CF) [Tzou's]
1	0.335	0.331
2	0.502	0.487
3	0.614	0.603
4	0.709	0.756
5	0.793	0.721
6	0.869	0.833
7	0.938	0.913
8	1.003	1.034
9	1,064	1.078
10	1.122	1.176

Table 6: Numerical inversion Laplace transform for Nusselt number by Stehfest's and Tzou's

P_{reff}	Nu (ABC) [Stehfest's]	Nu (ABC) [Tzou's]
1	0.478	0.452
2	0.544	0.523
3	0.678	0.634
4	0.739	0.765
5	0.799	0.732
6	0.876	0.821
7	0.959	0.926
8	1.009	1.052
9	1.078	1.098
10	1.129	1.189

6 Conclusion

The basic purpose of this article was to investigate the effect of the simultaneous use of ramped velocity and ramped temperature conditions on MHD Maxwell fluid. It is difficult to calculate the solutions of MHD Maxwell fluid using both ramp conditions. Fractional differential operators are used to finding solutions using Laplace transformation and inversion algorithm. Some comparisons have been drawn and they are in good agreement with the results published in [22,26,27]. The important finding of this investigation are:

- The velocity decreases by magnifying the value of the magnetic profile.
- The velocity increases with increasing values of G_r .
- The Nusselt number describes that the heat transfer rate enhances with increasing thermal diffusivity.
- The velocity decreases by magnifying the value of the P_{reff} .
- ABC fractional derivative is more considerable as compared to the classical model and other fractional models.

Acknowledgement: The authors are highly thankful and grateful for generous support and facilities of this research work.

Funding Statement: Self supported by the authors.

Conflicts of Interest: The authors declare that they have no conflicts of interest to report regarding the present study.

References

1. Ghosh, A. K., Sana, P. (2009). On hydromagnetics flow of an Oldroyd-B fluid near a pulsating plate. *Acta Astronautica*, 64(2–3), 272–280. DOI 10.1016/j.actaastro.2008.07.016.
2. Nadeem, S., Mehmood, R., Akbar, N. S. (2013). Non-orthogonal stagnation point flow of a nano non-Newtonian fluid towards a stretching surface with heat transfer. *International Journal of Heat and Mass Transfer*, 57(2), 679–689. DOI 10.1016/j.ijheatmasstransfer.2012.10.019.
3. Sharmilaa, K., Kaleeswari, S. (2015). Dufour effects on unsteady free convection and mass transfer through a porous medium in a slip regime with heat source/sink. *International Journal of Scientific Engineering and Applied Science*, 1, 307–320.

4. Mohyuddin, M. R., Hayat, T., Mahomed, F., Asghar, S., Siddiqui, A. M. (2004). On solutions of some non-linear differential equations arising in Newtonian and non-Newtonian fluids. *Nonlinear Dynamics*, 35(3), 229–248. DOI 10.1023/B:NODY.0000027920.92871.99.
5. Vajravelu, K., Cannon, J., Rollins, D., Leto, J. (2002). On solutions of some non-linear differential equations arising in third grade fluid flows. *International Journal of Engineering Science*, 40(16), 1791–1805. DOI 10.1016/S0020-7225(02)00070-8.
6. Maxwell, J. C. (1867). On the dynamical theory of gases. *Philosophical Transactions of the Royal Society of London*, 157, 49–88. DOI 10.1098/rstl.1867.0004.
7. Fetecau, C., Fetecau, C. (2003). A new exact solution for the flow of a Maxwell fluid past an infinite plate. *International Journal of Non-Linear Mechanics*, 38(3), 423–427. DOI 10.1016/S0020-7462(01)00062-2.
8. Fetecau, C., Jamil, M., Fetecau, C., Siddique, I. (2009). A note on the second problem of Stokes for Maxwell fluids. *International Journal of Non-Linear Mechanics*, 44(10), 1085–1090. DOI 10.1016/j.ijnonlinmec.2009.08.003.
9. Jamil, M., Fetecau, C., Khan, N. A., Mahmood, A. (2011). Some exact solutions for helical flows of Maxwell fluid in an annular pipe due to accelerated shear stresses. *International Journal of Chemical Reactor Engineering*, 9(1), 1.
10. Iftikhar, N., Husnine, S. M., Riaz, M. B. (2019). Heat and mass transfer in MHD Maxwell fluid over an infinite vertical plate. *Journal of Prime Research in Mathematics*, 15, 63–80.
11. Fetecau, C., Fetecau, C. (2003). The Rayleigh-Stokes-problem for a fluid of Maxwellian type. *International Journal of Non-Linear Mechanics*, 38(4), 603–607. DOI 10.1016/S0020-7462(01)00078-6.
12. Vieru, D., Zafar, A. A. (2013). Some Couette flows of a Maxwell fluid with wall slip condition. *Applied Mathematics & Information Sciences*, 7(1), 209–219. DOI 10.12785/amis/070126.
13. Aman, S., Khan, I., Ismail, Z., Salleh, M. Z., Al-Mdallal, Q. M. (2017). Heat transfer enhancement in free convection flow of CNTs Maxwell nanofluids with four different types of molecular liquids. *Scientific Reports*, 7(1), 423. DOI 10.1038/s41598-017-01358-3.
14. Asif, N. A., Hammouch, Z., Riaz, M. B., Bulut, M. (2018). Analytical solution of a Maxwell fluid with slip effects in view of the Caputo-Fabrizio derivative. *The European Physical Journal Plus*, 133(7), 371. DOI 10.1140/epjp/i2018-12098-6.
15. Zafar, A. A., Riaz, M. B., Imran, M. A. (2018). Unsteady rotational flow of fractional Maxwell fluid in a cylinder subject to shear stress on the boundary. *Punjab University journal of Mathematics*, 50, 21–32.
16. Noor, N. F. (2012). Analysis for MHD flow of a Maxwell fluid past a vertical stretching sheet in the presence of thermophoresis and chemical reaction. *World Academy of Science, Engineering and Technology*, 64, 1019–1023.
17. Sobral, D. C. (2003). A new proposal to guide velocity and inclination in the ramp protocol for the Treadmill Ergometer. *Arquivos Brasileiros de Cardiologia*, 81, 48–53.
18. Bruce, R. A. (1956). Evaluation of functional capacity and exercise tolerance of cardiac patients. *Modern Concepts of Cardiovascular Disease*, 25, 321–326.
19. Myers, J., Bellin, D. (2000). Ramp exercise protocol for clinical and cardiopulmonary exercise testing. *Sports Medicine*, 30(1), 23–29. DOI 10.2165/00007256-200030010-00003.
20. Kundu, B. (2016). Exact analysis for propagation of heat in a biological tissue subject to different surface conditions for therapeutic applications. *Applied Mathematics and Computation*, 285, 204–216. DOI 10.1016/j.amc.2016.03.037.
21. Ahmed, N., Dutta, M. (2013). Transient mass transfer flow past an impulsively started infinite vertical plate with ramped plate velocity and ramped temperature. *International Journal of Physical Sciences*, 8, 254–263. DOI 10.5897/IJPS12.390.
22. Seth, G., Nandkeolyar, R., Ansari, M. S. (2011). Effect of rotation on unsteady hydromagnetic natural convection flow past an impulsively moving vertical plate with ramped temperature in a porous medium with thermal diffusion and heat absorption. *International Journal of Applied Mathematics and Mechanics*, 7, 52–69.

23. Seth, G., Sharma, R., Sarkar, S. (2015). Natural convection heat and mass transfer flow with hall current, rotation, radiation and heat absorption past an accelerated moving vertical plate with ramped temperature. *Journal of Applied Fluid Mechanics*, 8, 7–20.
24. Seth, G., Sarkar, S. (2015). MHD natural convection heat and mass transfer flow past a time dependent moving vertical plate with ramped temperature in a rotating medium with Hall effects, radiation and chemical reaction. *Journal of Mechanics*, 31(1), 91–104. DOI 10.1017/jmech.2014.71.
25. Tiwana, M. H., Mann, A. B., Rizwan, M., Maqbool, K., Javeed, S. et al. (2019). Unsteady magnetohydrodynamic convective fluid flow of Oldroyd-B model considering ramped wall temperature and ramped wall velocity. *Mathematics*, 7(8), 676. DOI 10.3390/math7080676.
26. Anwar, T., Khan, I., Kumam, P., Watthayu, W. (2019). Impacts of thermal radiation and heat consumption/generation on unsteady MHD convection flow of an Oldroyd-B fluid with ramped velocity and temperature in a generalized Darcy medium. *Mathematics*, 8(1), 130. DOI 10.3390/math8010130.
27. Anwar, T., Kumam, P., Watthayu, W. (2020). Influence of ramped wall temperature and ramped wall velocity on unsteady magnetohydrodynamic convective maxwell fluid flow. *Symmetry*, 3(3), 392. DOI 10.3390/sym12030392.
28. Shah, N. A., Mahsur, Y., Zafar, A. A. (2017). Unsteady free convection flow of viscous fluids with analytical results by employing time-fractional Caputo-Fabrizio derivative (without singular kernel). *European Physical Journal Plus*, 132(10), 138. DOI 10.1140/epjp/i2017-11711-6.
29. Riaz, M. B., Siddiqui, I., Saeed, S. T., Atangana, A. (2020). MHD Oldroyd-B fluid with slip condition in view of local and nonlocal kernels. *Journal of Applied and Computational Mechanics*, 6(SI), 1540–1551.
30. Saeed, S. T., Riaz, M. B., Baleanu, D., Abro, K. A. (2020). A mathematical study of natural convection flow through a channel with non-singular kernels: An application to transport phenomena. *Alexandria Engineering of Journal*, 59(4), 2269–2281. DOI 10.1016/j.aej.2020.02.012.
31. Khan, I., Saeed, S. T., Riaz, M. B., Abro, K. A., Husnine, S. M. et al. (2020). Influence in a Darcy's medium with heat production and radiation on mhd convection flow via modern fractional approach. *Journal of Material Research and Technology*, 9(5), 10016–10030. DOI 10.1016/j.jmrt.2020.06.059.
32. Caputo, M., Fabrizio, M. (2016). Applications of new time and spatial fractional derivatives with exponential kernels. *Progress in Fractional Differentiation and Applications*, 2(1), 1–11. DOI 10.18576/pfda/020101.
33. Atangana, A., Baleanu, D. (2016). New fractional derivative with non local and non-singular kernel: Theory and application to heat transfer model. *Thermal Science*, 20(2), 763–769. DOI 10.2298/TSCI160111018A.
34. Riaz, M. B., Saeed, S. T., Baleanu, D. (2020). Role of magnetic field on the dynamical analysis of second grade fluid: An optimal solution subject to non-integer differentiable operators. *Journal of Applied and Computational Mechanics*, 6(SI), 1475–1489.
35. Riaz, M. B., Saeed, S. T., Baleanu, D., Ghalib, M. (2020). Computational results with non-singular & non-local kernel flow of viscous fluid in vertical permeable medium with variant temperature. *Frontiers in Physics*, 8, 15. DOI 10.3389/fphy.2020.00275.
36. Riaz, M. B., Saeed, S. T. (2020). Comprehensive analysis of integer order, Caputo–Fabrizio and Atangana–Baleanu fractional time derivative for MHD Oldroyd-B fluid with slip effect and time dependent boundary condition. *Discrete Continuous & Dynamical System*, DOI 10.3934/dcdss.2020430.
37. Imran, M. A., Aleem, M., Riaz, M. B., Ali, R., Khan, I. (2018). A comprehensive report on convective flow of fractional (ABC) and (CF) MHD viscous fluid subject to generalized boundary conditions. *Chaos Solitons Fractals*, 118, 274–289. DOI 10.1016/j.chaos.2018.12.001.
38. Riaz, M. B., Atangana, A., Saeed, S. T. (2020). MHD free convection flow over a vertical plate with ramped wall temperature and chemical reaction in view of non-singular kernel. *Fractional Order Analysis: Theory, Methods and Applications*. pp. 253–282. DOI 10.1002/9781119654223.ch10.
39. Riaz, M. B., Atangana, A., Iftikhar, N. (2020). Heat and mass transfer in Maxwell fluid in view of local and non-local differential operators. *Journal of Thermal Analysis and Calorimetry*. DOI 10.1007/s10973-020-09383-7.

40. Riaz, M. B., Iftikhar, N. (2020). A comparative study of heat transfer analysis of MHD Maxwell fluid in view of local and non-local differential operators. *Chaos, Solitons & Fractals*, 132, 109556. DOI 10.1016/j.chaos.2019.109556.
41. Khan, I., Shah, N. A., Mahsud, Y., Vieru, D. (2017). Heat transfer analysis in a Maxwell fluid over an oscillating vertical plate using fractional Caputo–Fabrizio derivatives. *European Physical Journal Plus*, 132(4), 513. DOI 10.1140/epjp/i2017-11456-2.
42. Khan, I., Ali, F., Shafie, S. (2013). Exact solutions for unsteady magnetohydrodynamic oscillatory flow of a Maxwell fluid in a porous medium. *Zeitschrift für Naturforschung A*, 68(10–11), 635–645. DOI 10.5560/zna.2013-0040.
43. Imran, M. A. (2020). Fractional mechanism with power law (singular) and exponential (non-singular) kernels and its applications in bio heat transfer model. *International Journal of Heat and Technology*, 37, 846–852.
44. Ahmed, M., Imran, M. A., Aleem, M., Khan, I. (2019). A comparative study and analysis of natural convection flow of MHD non-Newtonian fluid in the presence of heat source and first-order chemical reaction. *Journal of Thermal Analysis and Calorimetry*, 137(5), 1783–1796. DOI 10.1007/s10973-019-08065-3.
45. Aleem, M., Imran, M. A., Ahmadian, A., Salimi, M., Ferrara, M. (2020). Heat transfer analysis of channel flow of MHD Jeffrey fluid subject to generalized boundary conditions. *European Physical Journal Plus*, 135(1), 1. DOI 10.1140/epjp/s13360-019-00071-6.
46. Imran, M. A., Aleem, M., Ahmadian, A., Salahshour, S., Ferrara, M. (2020). New trends of fractional modeling and heat and mass transfer investigation of (SWCNTs and MWCNTs)-CMC based nanofluids flow over inclined plate with generalized boundary conditions. *Chinese Journal of Physics*, 66, 497–516. DOI 10.1016/j.cjph.2020.05.026.
47. Khan, M. N., Nadeem, S., Muhammad, N. (2020). Micropolar fluid flow with temperature-dependent transport properties. *Heat Transfer*, 49(4), 1–15.
48. Nadeem, S., Kiani, M. N., Saleem, A., Issakhov, A. (2020). Microvascular blood flow with heat transfer in a wavy channel having electroosmotic effects. *Electrophoresis*, 2020, 1–9, 2020.
49. Stehfest, H. A. (1970). Numerical inversion of Laplace transforms. *Communications of the ACM*, 13, 9–47.
50. Tzou, D. Y. (1970). *Macro to microscale heat transfer: The lagging behaviour*. Washington: Taylor and Francis.